Nuclear Instruments and Methods in Physics Research A 787 (2015) 270–274

Contents lists available at ScienceDirect

Nuclear Instruments and Methods in Physics Research A

journal homepage: www.elsevier.com/locate/nima

Amplitude and timing properties of a Geiger discharge in a SiPM cell

E. Popova [a,*], P. Buzhan [a], A. Pleshko [a], S. Vinogradov [b,c], A. Stifutkin [a], A. Ilyin [a], D. Besson [a,d], R. Mirzoyan [e]

[a] National Research Nuclear University MEPhI (Moscow Engineering Physics Institute), 115409, Kashirskoe Shosse 31, Russia
[b] University of Liverpool and Cockcroft Institute, Sci-Tech Daresbury, Keckwick Lane, Warrington WA4 4AD, Cheshire, UK
[c] P.N. Lebedev Physical Institute of the Russian Academy of Sciences, Leninskiy Prospect 53, Moscow 119991, Russia
[d] Department of Physics and Astronomy, University of Kansas, Lawrence, KS 66045-2151, USA
[e] Max-Planck-Institute for Physics, Föhringer Ring 6, 80805 München, Germany

ARTICLE INFO

Available online 22 December 2014

Keywords:
SiPM
Avalanche
Geiger discharge
Time resolution
Probability distribution

ABSTRACT

The amplitude and timing properties of a Geiger discharge in a stand-alone SiPM cell have been investigated in detail. Use of a single stand-alone SiPM cell allows us to perform measurements with better accuracy than the multicell structure of conventional SiPMs. We have studied the dependence of the output charge and amplitude from an SiPM cell illuminated by focused light vs the number of primary photoelectrons. We propose a SPICE model which explains the amplitude over saturation (when the SiPM's amplitude is greater than the sum over all cells) characteristics of SiPM signals for more than one initial photoelectrons. The time resolutions of a SiPM cell have been measured for the case of single (SPTR) and multiphoton light pulses. The Full Width Half Max (FWHM) for SPTR has been found to be at the level of 30 ps for focused and 40 ps for unfocused light (100 μm cell size).

1. Introduction

Silicon Photomultipliers (SiPM) are intrinsically very fast photodetectors because the Geiger discharge inside a tiny depletion region has very fast build-up and quench times.

However, the single photon time resolution (SPTR) of a 3 × 3 mm^2 SiPM for unfocused light (~200 ps, left scale of Fig. 1) is much worse than that of a single stand-alone SiPM cell of identical topology using a 2 μm light spot focused on the center of the cell (~30 ps, right scale of Fig. 1) [1].

Thus we studied the SPTR distribution of a single stand-alone cell to observe the time structure of a Geiger discharge development more clearly and deeply than is otherwise possible with a conventional multicell SiPM. Studies of a stand-alone cell also allow us to clarify recently observed oversaturation behavior of SiPM amplitude signals [2], which seems to be in contradiction with the well-known saturation model of SiPM's, at short laser pulse detection, based on the assumption of binary cell operations and the expected binomial statistics of fired cells:

$$n = N \times \left[1 - \exp\left(-\frac{N_{phot} \times \mathrm{PDE}}{N}\right)\right] \quad (1)$$

where N is the total number of cells inside the SiPM, n is the number of fired cells, N_{phot} is the number of photons and PDE is the light detection efficiency of a SiPM.

2. Amplitude and timing properties of a Geiger discharge in a SiPM cell

2.1. SPICE model of a Geiger discharge development

A Geiger discharge development determines the amplitude and timing properties of a SiPM. An SiPM single cell signal is a function of the discharge process itself and an SiPM's distributed electrical parameters (the cell's and parasitic capacitance, resistance, inductance) including the cell interconnection realization.

As far as we know, thus far no SPICE model for the simulation of a Geiger discharge development in an SiPM cell exists in the literature. The standard approach is to use Corsi SiPM model [3], employing a current source as a Dirac delta impulse to simulate the avalanche process. However, model does not correctly reproduce the rising edge of a SiPM cell pulse [4,5].

The scenario for the Geiger discharge development in an SPAD cell has been proposed in [6]. According to this approach the Geiger discharge in an SiPM cell begins after the appearance of free carriers (electron–hole pairs) in the high field zone of a depletion region from a submicron initial spot with a longitudinal build-up of the avalanche process. During this phase, the local spot current, after a certain

* Corresponding author. Tel.: +7 910 418 8464; fax: +7 499 324 7105.
E-mail address: elenap73@mail.ru (E. Popova).

http://dx.doi.org/10.1016/j.nima.2014.12.050
0168-9002/

number of generations of ionization events, reaches quasi-stationary conditions which are themselves determined by the overvoltage applied to this spot. The discharge then expands by extending to boundary regions due to multiplication-assisted diffusion (Fig. 2).

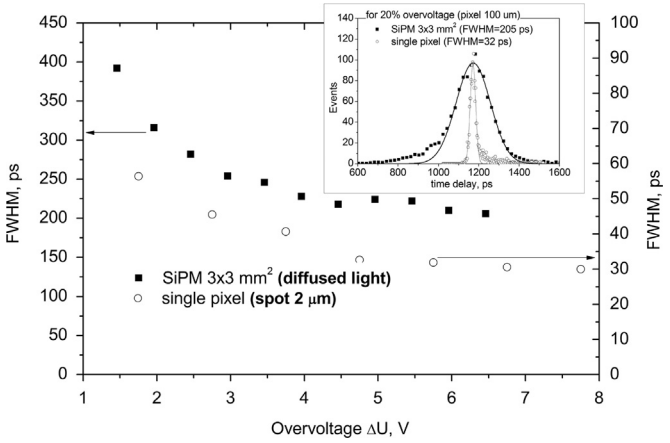

Fig. 1. SPTR for 3×3 mm^2 SiPM and single standalone cell with equal topology and 100×100 μm^2 cell size (20% V_{ov}).

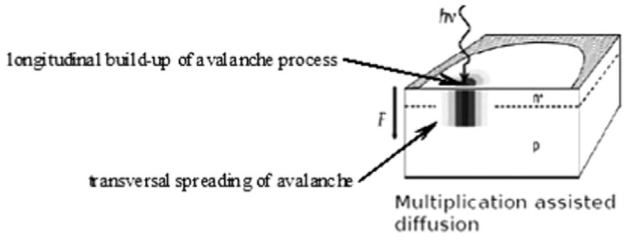

Fig. 2. Models of discharge propagation in a SPAD.

This lateral expansion lasts as long as the $p-n$ junction overvoltage supports continued ionization (note that the overvoltage inevitably drops due to discharge of a cell's capacitor by the avalanche current). According to results obtained by our group using light emission microscopy, the discharge spot is spread out to a lateral scale of approximately 10 μm [7].

All these processes are incorporated in the Dolgoshein–Pleshko Geiger discharge lateral development SPICE model (Fig. 3):

- A Geiger discharge starts from an elementary spot ("start disk") inside a cell.
- Within the start disk, a carrier density equal to $J_0 = k_J \times V_{ov}^0$ is established, where $V_{ov}^0 = V_{ov}(t=0)$ is the initial overvoltage. The parameter k_J may be physically interpreted in terms of the space-charge conductivity per junction area unit [6].
- Space charge effects uniformly lower the electric field inside the cell owing to the very small spreading resistance of the cell surfaces.
- The overvoltage V_{ov}^1 at time $t_1 > 0$ falls below V_{ov}^0.
- At the same time (t_1) the 1st elementary ring begins to fire. Its current density (and disk current density at the time moment t_1) assumes the value $J_1 = k_J \times V_{ov}^1 < k_J \times V_{ov}^0$.
- The process then repeats itself, until the overvoltage and the cell current falls to zero 0. During this process, the instantaneous current density is given by $J(t) = k_J \times V_{ov}(t)$.
- The discharge spreads from the spot with velocity $u(t) = u_0 \times V_{ov}(t)/\ V_{ov}^0$. Here u_0 is the initial velocity, which is independent of the initial overvoltage. This velocity relationship agrees with the current experimental data, according to which the final spot size is independent of the initial overvoltage [7].

Using these relations for the specific current density and lateral speed, it is straightforward to obtain an expression for the total cell current:

$$I(t) = J(t)S(t) = J(t) \times \pi r^2(t) = \pi k_J V_{ov}(t) \left[\int_0^t u_0 \frac{V_{ov}(t')}{V_{ov}^0} dt' \right]^2 \quad (2)$$

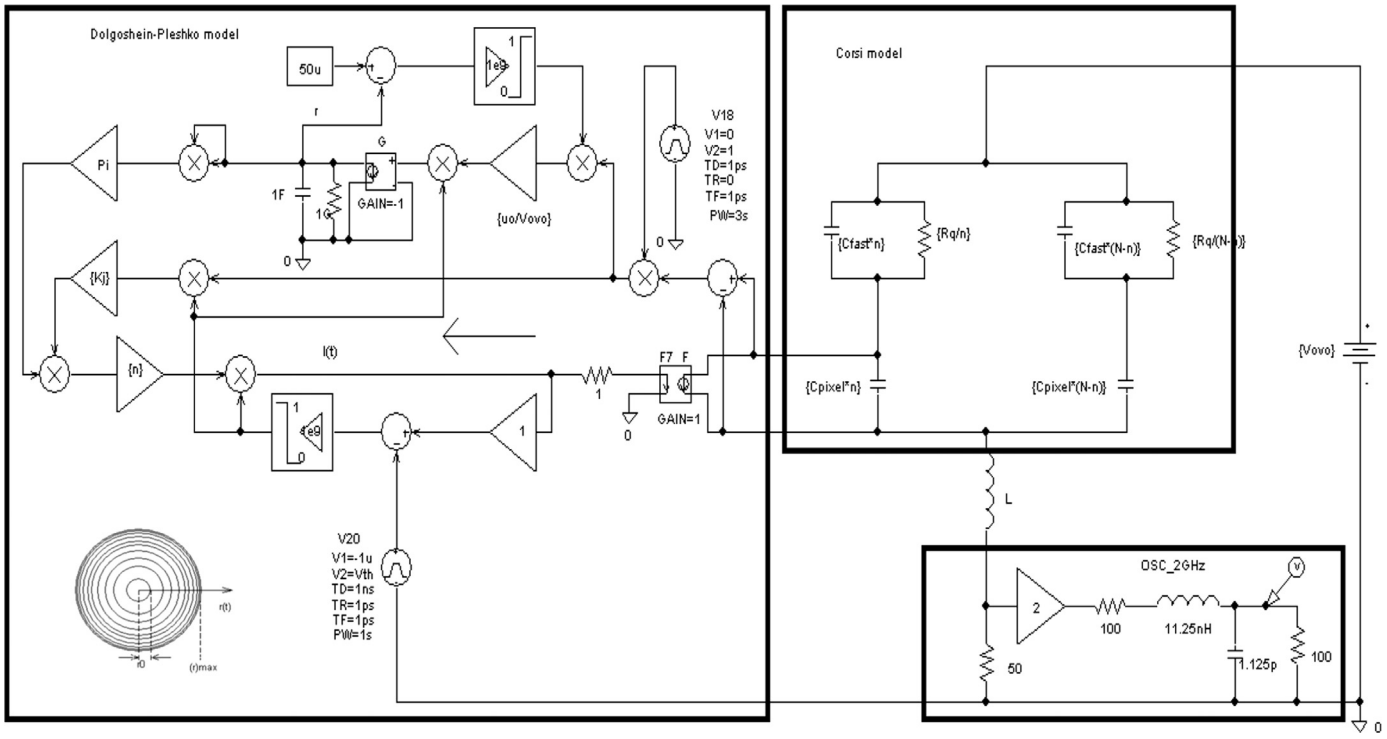

Fig. 3. Dolgoshein–Pleshko SPICE model for Geiger discharge in a SiPM cell.

On the basis of this expression and the values of the electrical SiPM parameters (extracted as described in [8]), a SPICE model simulation block of a Geiger discharge lateral development was written.

2.2. Comparison of model prediction and experimental waveforms

For our study we have used single cell $100 \times 100\ \mu m^2$ produced in Zelenograd, (Russia) as a test structure in the SiPM batch described in [1]. A pulsed laser source with 40 ps FWHM pulse duration ($\lambda = 660$ nm) has been focused into a 10 μm spot at the cell center. As mentioned above, the Geiger discharge spot is located in the central part of the cell and does not reach the peripheral cell regions. The light intensity is modulated by neutral density filters from a single photon to approximately one hundred photons. The applied voltage $U = 35$ V (Ubreakdown = 33.5 V). Signals have been recorded directly by a digital oscilloscope LeCroy WaveRunner 620Zi, with 2 GHz analog bandwidth (input impedance 50 Ω, DC).

Our SPICE model (Fig. 3) has been used with $N = n = 1$ (one firing cell, one cell in total) but with a varying number of Geiger discharge blocks, as described in Section 2.1, connected in parallel and simulating different number of starting spots (photoelectrons) in one cell.

Both the model (Fig. 4) and the experiment (Fig. 5) show similar single cell waveform behavior for one initial photoelectron and for many photoelectrons initiating avalanches in different points simultaneously; these points correspond the position of the light spot in the cell. For many photoelectrons the amplitude is much higher and pulse duration is shorter. However, the total charge of the fired cell remains the same. These results support the explanation of amplitude over saturation as given in [2].

3. The timing resolution of a SiPM cell

The time resolution of a SiPM cell was measured with the digital oscilloscope LeCroy WaveRunner 620Zi, in conjunction with a FEMTO-T laser system (pulse width 176 fs FWHM and $\lambda = 876$ nm [9]). Time stamp was generated by the oscilloscope used as both a leading edge discriminator (at a minimally detectable constant threshold level) and TDC. The dependence of SPTR vs overvoltage has a decay (up to 4.5 V) and a plateau (higher then 4.5 V) at the level of 30 ps FWHM for light focused into a 2 μm spot (Fig. 1, circles). We assume that at low overvoltages the SPTR is defined mostly by a vertical build-up of the

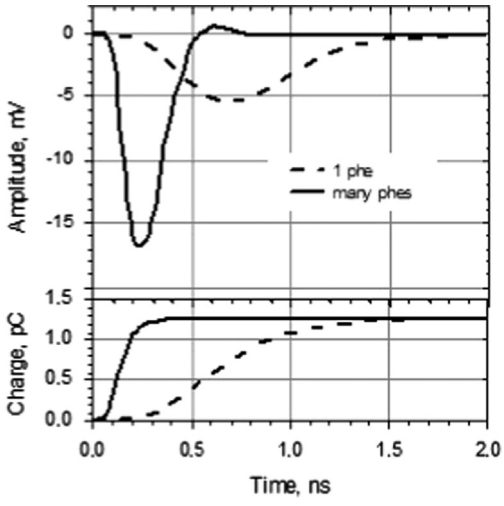

Fig. 4. SPICE simulated pulses and total charge for one SiPM cell in case of single phe (dashed lines) and 100 phe (solid lines) initial spots.

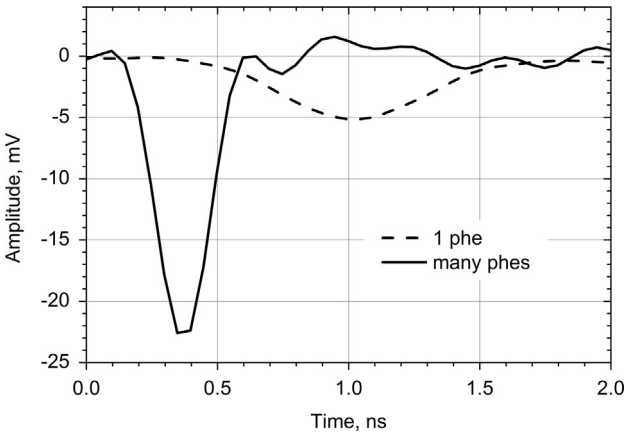

Fig. 5. Scope pulses for one SiPM cell in case of single phe (dashed line) and 100 phe (solid line) initial spots.

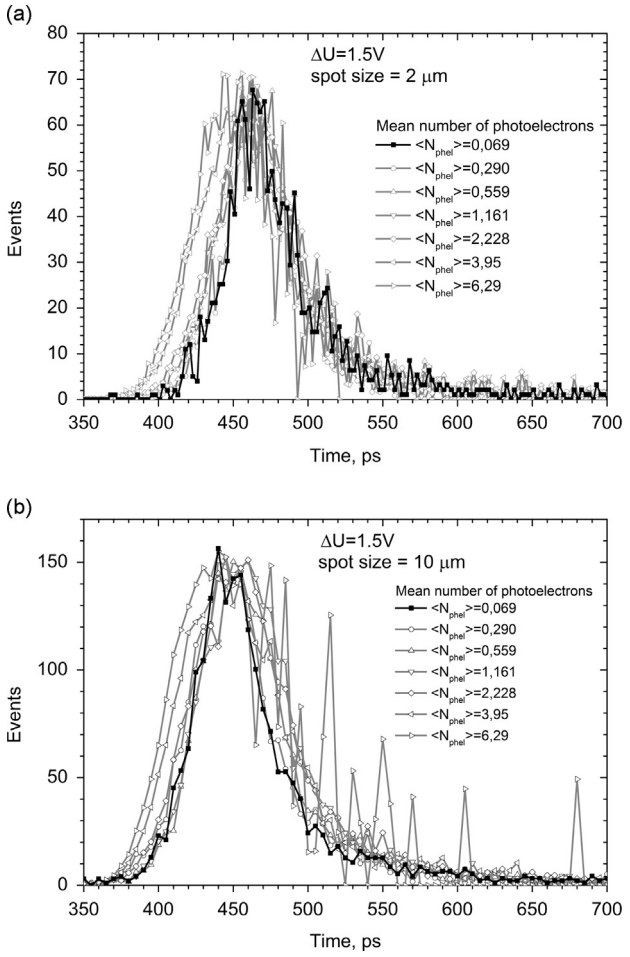

Fig. 6. Single SiPM cell reconstructed SPTR for 2 μm (a) and 10 μm (b) light spot for overvoltage 1.5 V and different mean number of initial phe (black dots – true SPTR).

Geiger discharge, and at high overvoltages it reaches a constant level determined by the lateral spreading of the discharge.

In order to prove this assumption the following experiment has been conducted. We have measured the SiPM cell time resolution for different intensity light focused to 2 and 10 μm spot sizes at the center of a SiPM cell for low and high overvoltages corresponding to the SPTR decay region and SPTR plateau region of Fig. 1. We believe that for 2 μm light spot we have one starting avalanche spot despite

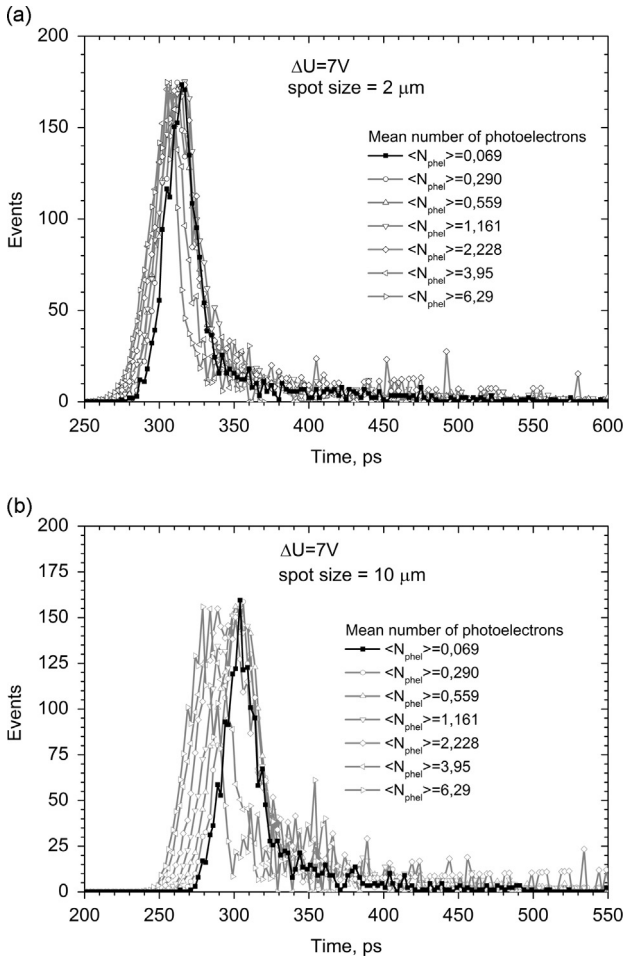

Fig. 7. Single SiPM cell reconstructed SPTR for 2 μm (a) and 10 μm (b) light spot for overvoltage 7 V and different mean number of initial phe (black dots – true SPTR).

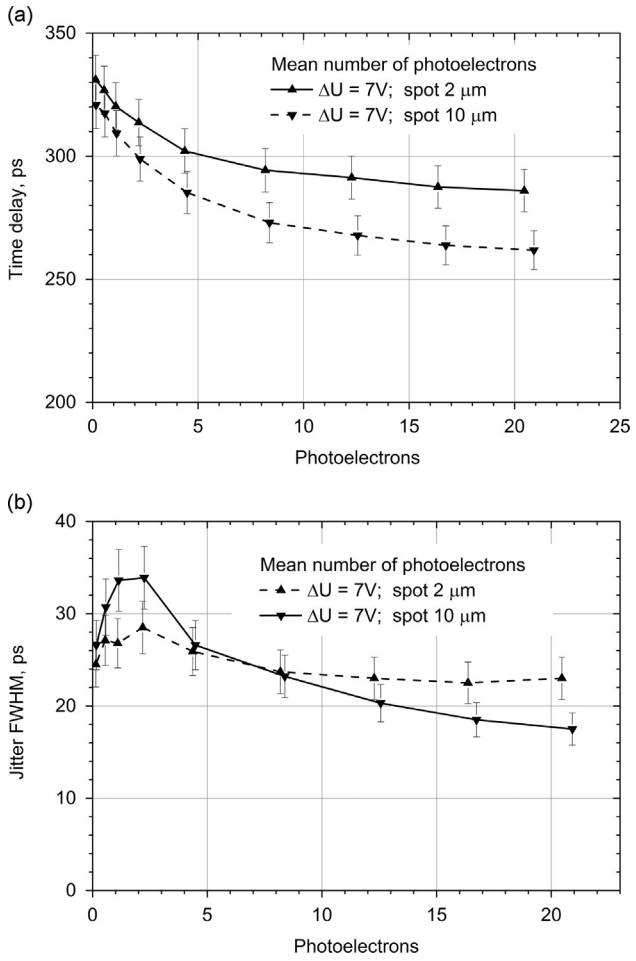

Fig. 8. Time delay (a) and jitter (b) of SiPM cell signal measured vs mean number of initial phes for light spot 2 μm and 10 μm for 7 V overvoltage.

the large number of primary photoelectrons, whereas for 10 μm and for light intensity more then 1 phes we should have several independent starting points similar to the conditions described in Section 2.2.

Studying time jitter dependence vs number of photoelectrons we account for the well known effect of the narrowing of the transit time distribution due to multiple possible photoelectron arrival times.

Using an approach described in [10] for the reconstruction of a true SPTR for a variable number of photoelectrons, we obtain the curves shown in Fig. 6 (overvoltage 1.5 V), and Fig. 7 (overvoltage 7 V) for laser spot size 2 μm (a) and 10 μm (b). Comparing the most probable values and the distribution widths on Figs. 6a and b and 7a and b we can see that the reconstruction procedure works acceptably until $\langle N\rangle = 2.2$ phe for Figs. 6a and b and 7a, but for overvoltage 7 V 10 μm spot size (Fig. 7b) starts to fail from the very beginning.

We assume that the vertical buildup process is the same for both spot sizes, and that, prior to lateral spreading, the timing jitter is determined by just the number of free carriers in high field region and is independent of their position (whether inside one avalanche spot or different spots). Although we might expect the same to hold true for the vertical development at high overvoltage, the considerable difference between Fig. 7a and b suggests that for the SPTR plateau region the lateral development plays a different role for one starting discharge point (2 μm) and several (10 μm). Thus, at even extremely low threshold values, the lateral contribution dominates over the vertical one for the plateau region. For overvoltage value of approximately 7 V the dependence of the most probable transit time delay on the mean number of starting Geiger discharge photoelectrons for 2 and 10 μm spot sizes is shown in Fig. 8a. The measured jitter is presented in Fig. 8b. Deterioration of resolution for mean phe values between 1 and 4 is attributed to the SiPM cell signal amplitude sensitivity to the number of carriers initiating the discharge, which fluctuates according to Poisson statistics for fixed mean value. Curves corresponding to 2 and 10 μm have different behaviour due to different contribution of lateral spreading process.

4. Conclusions

We have considered the true single electron response of a SiPM cell. In particular, we have studied how the amplitude of a multi-photoelectron pulse increases and the pulse width decreases with an increasing number of photoelectrons initiating the Geiger discharge. Within the observed range of photoelectrons, the total output charge is fixed at the single electron response value. The SPTR at low overvoltages is defined by a vertical build-up of the Geiger discharge, whereas at high overvoltages it approaches a plateau value defined by the lateral discharge development. Overall a single cell SPTR may be improved using low threshold triggering, combined with a low noise front-end preamplifier.

Acknowledgments

Work has been supported by Megagrant 2013 program of Russia Agreement 14.A12.31.0006 from 24.06.2013. This work has also been

supported in part by the EC under Grant agreement no. 329100 and the STFC Cockcroft Institute Core Grant no. ST/G008248/1.

References

[1] B. Dolgoshein, et al., Nuclear Instruments and Methods in Physics Research Section A 695 (2012) 4043.
[2] L. Gruber, et al., Nuclear Instruments and Methods in Physics Research Section A 737 (2014) 1118.
[3] F. Corsi, et al., Nuclear Instruments and Methods in Physics Research Section A 572 (2007) 416418.
[4] D. Marano, G. Bonanno, M. Belluso, et al., Nuclear Instruments and Methods in Physics Research Section A 726 (2013) 17.
[5] D. Marano, G. Bonanno, M. Belluso, et al., IEEE Transactions on Nuclear Science NS-61 (1) (2014) 23.
[6] A. Lacaita, M. Mastrapasqua, M. Ghioni, S. Vanoli, Applied Physics Letters 57 (1990) 489.
[7] E. Popova, et al., Simulation and measurements of Geiger discharge transverse size in a SiPM cell, in: Talk Given on 2013 IEEE NSS/MIC/RTSD, Seoul.
[8] A. Pleshko, P. Buzhan, E. Popova, et al., Instruments and Experimental Techniques 56 (N6) (2013) 697.
[9] A. Egorov, A. Chumakov, O. Mavritskiy, et al., Femtosecond laser simulation facility for SEE IC testing, in: Talk Given at IEEE Nuclear and Space Radiation Effects Conference, Paris, France, 2014, pp. 14–18.
[10] S. Vinogradov, et al., Journal of Instrumentation 6 (2011) P02013.